

Laboratory of Pharmacology and Toxicology¹, School of Pharmaceutical Sciences, Sun Yat-Sen University, Guangzhou; Shenzhen Institute for Drug Control², Shenzhen; Guangzhou Medical University³, Guangzhou, State Key Laboratory of Oncology⁴, Department of Neurosurgery, Cancer Center, Sun Yat-sen University, Guangzhou, China

Tanshinone IIA prevents cardiac remodeling through attenuating NAD (P)H oxidase-derived reactive oxygen species production in hypertensive rats

PING WANG^{*1,2}, XIAOQIAN WU^{*1,3}, YINGXIA BAO^{*1}, JIAN FANG¹, SIGUI ZHOU¹, JIE GAO¹, RONGBIAO PI¹, YONG-GAO MOU⁴, PEIQING LIU¹

Received October 2, 2010, accepted November 19, 2010

Dr. Peiqing Liu, Laboratory of Pharmacology and Toxicology, School of Pharmaceutical Sciences, Sun Yat-sen University, 132 Waihuan-Dong Road, Guangzhou 510006, China
liupq@mail.sysu.edu.cn

Dr. Yong-gao Mou, State Key Laboratory of Oncology, Department of Neurosurgery, Cancer Center, Sun Yat-sen University, Guangzhou 510060, China
mouyg@mail.sysu.edu.cn

*Both authors contributed equally to this work.

Pharmazie 66: 517–524 (2011)

doi: 10.1691/ph.2011.0806

Tanshinone IIA is one of major constituents of *Salvia miltiorrhiza* Bunge known as Danshen. Our and others' studies have shown that Tan IIA could protect cardiomyocyte against apoptosis; however the effect of Tan IIA on cardiac remodeling disease is still unknown. In this study, we investigated the effects of Tan IIA on cardiac hypertrophy and fibrosis in two-kidney, two-clip (2K2C) hypertensive rats and by which, if any, mechanisms. Administration of 2K2C hypertensive rats with Tan IIA attenuated cardiac dysfunction and fibrosis. However Tan IIA treatment had no effects on BP control. Further studies revealed that Tan IIA inhibited the increased NAD(P)H oxidase activity and expression as well as O₂^{•-} production in 2K2C hypertensive rats. Our results indicated that Tan IIA significantly improved cardiac function and attenuated fibrosis in 2K2C hypertensive rats. The protective action of Tan IIA is likely mediated by its antioxidant effect, independent of BP control, partially via inhibiting NADPH oxidase.

1. Introduction

Human renovascular disease is one of the most common causes of secondary hypertension. In this situation, the renin-angiotension system (RAS) is highly activated due to the decrease of the renal blood flow and perfusion pressure after renal artery stenosis (Minuz et al. 2002). The heart responds to the increased afterload by initiating adaptive myocardial remodeling, which are deleterious over time and eventually result in heart failure (Ertl and Frantz 2005; Jugdutt 2003). Myocardial remodeling is characterized by alterations in left ventricular size, shape and wall thickness (Weber 1997). Multiple factors may, in fact, contribute to left ventricular remodeling (Khaper et al. 2003; Lu et al. 2004). Growing evidence suggests that oxidative stress mediated by reactive oxygen species plays a role in the pathogenesis of myocardial remodeling. ROS modulate several processes underlying myocardial remodeling, including proinflammatory cytokine release, cardiomyocyte apoptosis and fibrogenesis (Hare 2001).

Vascular NAD(P)H oxidases, also known as nonphagocytic NAD(P)H oxidases, are the major enzymatic sources of ROS in the heart (Lambeth 2004; Nakagami et al. 2003). In contrast to the phagocyte NADPH oxidase, which uses NADPH exclusively as an electron donor, vascular NAD(P)H oxidase also consume NADH (Lassegue and Clempus 2003). NAD(P)H oxidase is composed by a membrane-bound heterodimer consisting a catalytic Nox2 subunit (also known as gp91^{phox}) and a p22^{phox}

subunit and several cytosolic subunits (p47^{phox}, p40^{phox}, p67^{phox} and Rac) that associate with the heterodimer in the activated enzyme. Five Nox isoforms (Nox1–5) form the basis of distinct NAD(P)H oxidase (Lambeth 2004; Nakagami et al. 2003). Recent studies suggested that NAD(P)H plays an essential role in the development of hypertension, cardiac hypertrophy and interstitial fibrosis (Murdoch et al. 2006). The Nox 2 containing NADPH oxidase was thought as the major isoform to take part in cardiac hypertrophy and interstitial fibrosis (Bendall et al. 2002).

Tanshinone IIA (Tan IIA) is the main active diterpene quinone extracted from the traditional herbal drug, *Salvia miltiorrhiza* Bunge, known as “Danshen”. Sodium tanshinone IIA sulfonate (STS), a derivative of Tan IIA, is widely used in China for the treatment of cardiovascular diseases. Clinical evidence has shown that STS increases coronary blood flow, alleviates cardiac metabolic disorders, protects the heart against ischemia-reperfusion injury and attenuates atherosclerosis (Zhou et al. 2003). Recent studies have shown that STS markedly suppressed Ang II-induced enlargement of cultured myocytes and Tan IIA inhibited the basic fibroblast growth factor (bFGF)-induced human smooth muscle cell (SMC) proliferation in a dose-dependent manner (Takahashi et al. 2002). Our studies have shown that Tan IIA can inhibit atherosclerotic calcification mediated by decreasing the oxidation of LDL and protect cardiac myocytes against apoptosis due to its antioxidant properties (Fu et al. 2007; Tang et al. 2007). However, the role of Tan IIA

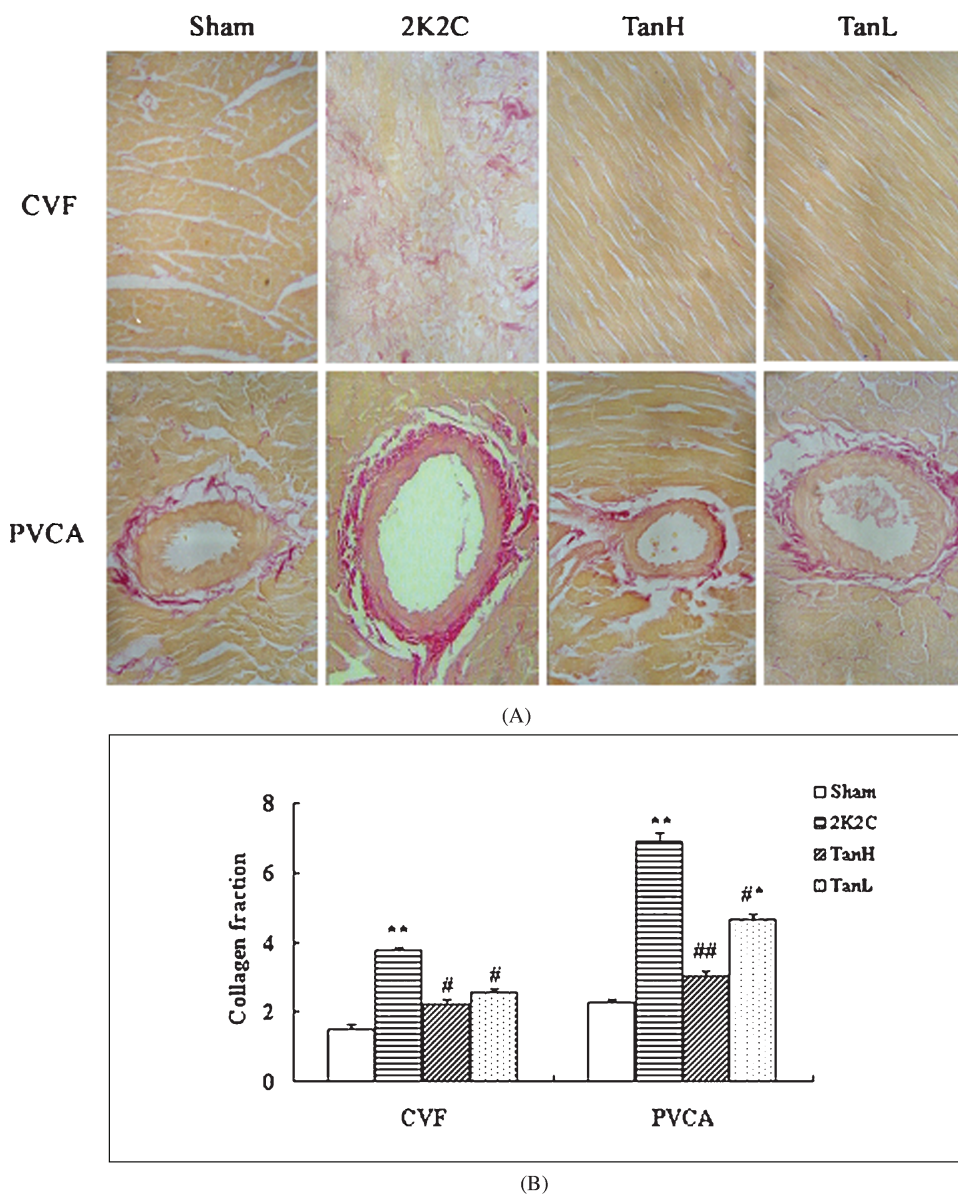


Fig. 1: Tanshinone IIA attenuated myocardial fibrosis in 2K2C rats. (A) Representative pictures of myocardial and perivascular fibrosis with the collagen-specific dye method VanGieson (VG) staining, in which collagen fibers appeared as red structures, and myocytes and intramyocardial vessels were yellow (magnification $\times 20$); (B) Collagen deposition in the interstitial and perivascular regions of the LV, expressed as collagen volume fraction (CVF) and perivascular collagen area (PVCA) measured by videodensitometry. Data are means \pm SD. $n = 10$. * $p < 0.05$ vs. Con. # $p < 0.05$ vs. Mod. Sham, sham-operation group; 2K2C, 2K2C-operation group; Tan H, high dose of Tan IIA (70 mg/kg/day); Tan L, low dose of Tan IIA (35 mg/kg/day)

in cardiac remodeling in the situation of renovascular disease remains unclear. Therefore, we investigated the effects of Tan IIA on two-kidney, two-clip (2K2C) renovascular hypertension-induced cardiac hypertrophy and fibrosis in rats. Further, we investigated whether the anti-oxidative activities of Tan IIA is related to NAD(P)H oxidase, if any, by which Nox isoform.

2. Investigations and results

2.1. Characterization of cardiac hemodynamic parameters and the effect of tanshinone IIA

To investigate the effect of tanshinone IIA on cardiac hypertrophy we established a two-kidney, two-clip (2K2C) model and examined cardiac hemodynamic parameters in rats. LVW/BW, the ratio of left ventricle weight (LVW) to body weight (BW), was analyzed as a surrogate marker of hypertension-induced left ventricular hypertrophy (Table 1). Compared with the Sham rats, LVW/BW in 2K2C rats was significantly increased to 159% ($P < 0.05$, $n = 12$), while there was no significant difference of BW among parallel groups (data not shown). The

value of LVW/BW was significantly lower in 2K2C+TanH rats (2.40 ± 0.17) than the BW-matched 2K2C rats (3.05 ± 0.18). Our result showed that high dose of TAN IIA treatment decreased the value of LVW/BW ratio in 2K2C rats.

In addition, we cannulated the right carotid artery to the LV before sacrifice by the end of 10 weeks to obtain hemodynamic data (Table 2). Compared with Sham rats, the left ventricle systolic pressure (LVSP) and the left ventricle end-diastolic pressure (LVEDP) were increased significantly in 2K2C hypertensive rats, which indicated that both preload and afterload were increased. Correspondingly, the maximum ascending and declining rate of left ventricular pressure ($\pm dp/dt_{max}$) were increased significantly in 2K2C hypertensive rats ($P < 0.05$, $n = 12$), indicating that contractility and diastolic compliance of the heart were decreased. Compared with 2K2C rats, the value of LVEDP and $\pm dp/dt_{max}$ were significantly decreased in 2K2C+TanH rats ($P < 0.05$, $n = 12$), which exhibited improvement of the left ventricular systolic function and diastolic compliance. However, the values of LVSP and $\pm dp/dt_{max}$ of 2K2C+TanH were still much higher than in 2K2C rats, indicating that the high afterload still remained. In addition, there was no sig-

Table 1: Characteristics of the animals

	Sham	2K2C	TanH	TanL
n	14	13	14	13
LVW/BW(mg/g)	1.8 ± 0.13	3.05 ± 0.18*	2.4 ± 0.17#	2.7 ± 0.20*
BP1(mmHg)	123 ± 5	121 ± 4	122 ± 3	122 ± 3
BP2(mmHg)	126 ± 4	177 ± 6*	180 ± 7*	181 ± 5*
BP3(mmHg)	125 ± 5	189 ± 7*	177 ± 5*	186 ± 3*
HR	414 ± 18	441 ± 15*	429 ± 22	438 ± 19

Data are means ± SD. n, number of rats in individual group. LVW/BW3, ratio of left ventricle weight to body weight after treatment at week 10; BP1, blood pressure before operation; BP2, blood pressure after hypertension developed and before treatment at week 4; BP3, blood pressure after treatment at week 10; Sham, sham-operation group; 2K2C, 2K2C-operation group; TanH, 2K2C hypertensive rats treated with Tan IIA at 70 mg/kg/day; TanL, 2K2C hypertensive rats treated with Tan IIA at 35 mg/kg/day. * $p < 0.05$ vs. sham group. # $p < 0.05$ vs. 2K2C group.

Table 2: Changes in cardiac hemodynamic parameters

	Sham	2K2C	TanH	TanL
n	14	13	14	13
LVSP	143 ± 16	186 ± 18*	175 ± 8*	182 ± 13*
LVEDP	5.3 ± 0.6	9.2 ± 0.7*	6.3 ± 0.5#	7.1 ± 0.9
+dp/dtmax	5.21 ± 0.31	9.78 ± 0.43*	7.31 ± 0.32#*	8.28 ± 0.51*
-dp/dtmax	4.39 ± 0.36	9.61 ± 0.39*	6.47 ± 0.22#*	7.15 ± 0.23#*

Data are means ± SD. n, number of rats in individual group. LVSP(mmHg), left ventricle systolic pressure; LVEDP(mmHg), left ventricle end-diastolic pressure; +dp/dtmax(mmHg/ms), maximum ascending rate of left ventricular pressure; -dp/dtmax, maximum declining rate of left ventricular pressure. Sham, sham-operation group; 2K2C, 2K2C-operation group; TanH, 2K2C hypertensive rats treated with Tan IIA at 70 mg/kg/day; TanL, 2K2C hypertensive rats treated with Tan IIA at 35 mg/kg/day. * $p < 0.05$ vs. sham group. # $p < 0.05$ vs. 2K2C group.

nificant difference of LVEDP, LVSP and + dp/dtmax between 2K2C+TanL rats and 2K2C rats, except that - dp/dtmax. Subsequently, high dose of Tan IIA exhibited a much more remarkable improvement of cardiac systolic and diastolic function.

Despite the fact that Tan IIA treatment ameliorated cardiac hemodynamic overload in 2K2C rats, it did not control blood pressure (BP) as shown in Table 1. BP was increased significantly in a time-dependent manner to an average of 189 mmHg by the end of 10 weeks in 2K2C rats compared with Sham rats ($P < 0.05$, $n = 12$). However, neither high nor low dose of Tan IIA treatment for six weeks reduced BP compared to that of 2K2C hypertensive rats ($P > 0.05$, $n = 12$). These results indicated that Tan IIA treatment might exert cardioprotective effects independent of BP control.

2.2. Characterization of cardiac dysfunction estimated by echocardiographic studies and the effect of tanshinone IIA

In order to confirm the beneficial effect of Tan IIA on cardiac hemodynamics, we further performed echocardiographic studies. The echocardiographic data are shown in Table 3. The values of interventricular septum end-diastolic thickness (IVSd), left ventricular posterior wall end-diastolic thickness (PWd), interventricular septum end-systolic thickness (IVSs), left ventricular end-systolic dimension (LVDs) and left ventricular posterior wall end-systolic thickness (PWs), increased while others, including left ventricular end-diastolic dimension (LVDd), ejection fraction (EF) and left ventricular fraction shortening (LVFS), decreased significantly ($p < 0.05$) in 2K2C rats compared with those in Sham group, indicating that the 2K2C rats developed obvious concentric cardiac hypertrophy and that compliance of myocardium was deteriorated especially in diastolic phase. Treatment with Tan IIA significantly delayed the cardiac hypertrophy development and the deterioration of cardiac function estimated by the decreased parameters such as IVSd, PWd, IVSs, LVDs and PWs, and the increased LVDd, EF, LVFS, compared with untreated 2K2C rats. There was no significant difference of those parameters between individual groups before operation and before treatment, and the data were not shown.

2.3. Tanshinone IIA attenuated myocardial fibrosis in 2K2C rats

To explore the mechanism by which Tan IIA improved cardiac hemodynamics, we further investigated the effect of Tan IIA on cardiac remodeling. Myocardial fibrosis was evaluated by two independent methods: morphometrically by staining of collagen volume fraction (CVF) and perivascular collagen area (PVCA). As shown in Fig. 1, diffused interstitial and perivascular fibrosis were evident in 2K2C hypertensive rats, which were demonstrated by collagen volume fraction (CVF) and perivascular collagen area (PVCA) respectively. Administration of Tan IIA (35,70 mg/kg) treatment for 6 weeks dose-dependently decreased CVF and PVCA, which indicates that Tan IIA treatment attenuated myocardial fibrosis both in the interstitium and perivascular areas.

2.4. Tanshinone IIA decreased $O_2^{\bullet-}$ generation

There is increasing evidence showing that oxidative stress is implicated in the development of cardiac remodeling. To investi-

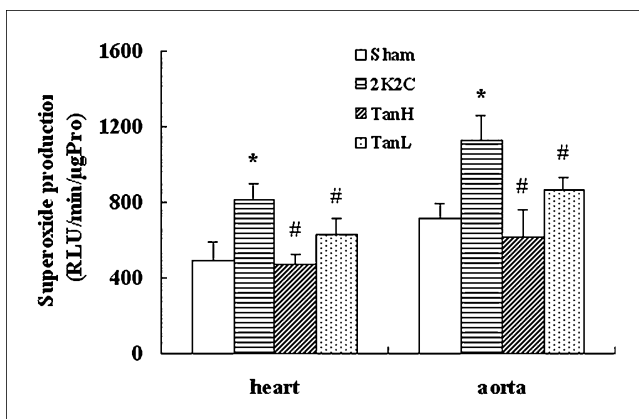


Fig. 2: Changes of $O_2^{\bullet-}$ production in LV and aorta homogenates determined by chemiluminescence of lucigenin in 2K2C hypertensive rats and the effect of Tan IIA. RLU, relative light units. Other abbreviations as above. Data are expressed as means ± SD. * $p < 0.05$ vs. Con. # $p < 0.05$ vs. Mod. $n = 6$

Table 3: Tanshinone IIA improved cardiac hypertrophy and dysfunction estimated by echocardiography

	Sham	2K2C	TanH	TL
IVSd	1.49 ± 0.12	2.68 ± 0.25*	1.82 ± 0.18*#	1.95 ± 0.19*#
LVDd	4.96 ± 0.11	4.23 ± 0.07*	4.75 ± 0.12#	4.64 ± 0.11#
PWd	1.53 ± 0.08	3.31 ± 0.17*	2.06 ± 0.16#	2.17 ± 0.12#
IVSs	2.14 ± 0.16	4.08 ± 0.13*	2.89 ± 0.12#	3.40 ± 0.11*
LVDs	1.07 ± 0.06	1.99 ± 0.14*	1.50 ± 0.21#	1.71 ± 0.15*
PWs	2.55 ± 0.16	4.24 ± 0.26*	3.06 ± 0.21#	3.31 ± 0.43
EF%	86.53 ± 1.48	65.23 ± 1.47*	84.08 ± 2.73#	79.50 ± 1.38*#
LVFS%	58.43 ± 1.38	40.29 ± 1.46*	54.70 ± 2.90#	49.35 ± 1.32*#

Data are means ± SD. n = 10. IVSd, interventricular septum end-diastolic thickness; LVDd, left ventricular end-diastolic dimension; PWd, left ventricular posterior wall end-diastolic thickness; IVSs, interventricular septum end-systolic thickness; LVDs, left ventricular end-systolic dimension; PWs, left ventricular posterior wall end-systolic thickness; EF, ejection fraction; LVFS, left ventricular fraction shortening. Other abbreviations as in Table 2. * $p < 0.05$ vs. Sham group. # $p < 0.05$ vs. 2K2C group.

Table 4: Primers sequence of NAD(P)H oxidase subunits

Transcript	Sense (5'-3')	Antisense (5'-3')	Product size (bp)	Accession No.
p47phox	S-CCA CAC CTC TTG AAC TTC	A- GCC ATC TAG GAG CTT ATG	453	AF260779
Nox2	S-TAT TGT GGG AGA CTG GAC TG	A- GAT TGG CCT GAG ATT CAT CC	401	AY174116
Nox4	S-GTT CCA AGC TCA TTT CCC AC	A- GTA TCG ATG CAA ACG GAG TG	500	NM_053524
β-actin	S-AGC CAT GTA CGT AGC CAT CC	A- CTC TCA GCT GTG GTG GTG AA	228	NM_031144

gate the mechanism by which Tan IIA attenuated cardiac fibrosis and improved the hemodynamics we examined its effect on $O_2^{\bullet-}$ Generation.

As shown in Fig. 2, the superoxide anion production by the LV and aorta were significantly increased to 168% and 158%, respectively, in 2K2C hypertensive rats compared with Sham rats ($P < 0.05$, n = 6), detected by lucigenin-enhanced chemiluminescence assay. Tan IIA treatment for 6 weeks dose-dependently decreased in $O_2^{\bullet-}$ levels in both aorta and LV compared to 2K2C rats.

2.5. Tanshinone IIA inhibited NAD(P)H oxidase activity in 2K2C rats

It was reported that NAD(P)H oxidase is the major enzymic resource of ROS in cardiovascular disease. We performed

a lucigenin-enhanced chemiluminescence assay to examine NAD(P)H oxidase activity of the heart and the aorta. NADH and NADPH oxidase activities in aorta and NADH oxidase in the LV were increased in the 2K2C group than those in Sham group. Tan IIA treatment dose-dependently reduced the activity of both of these two enzymes (Fig. 3). Interestingly, NADPH oxidase activity in the LV showed no significant change among individual groups, which indicated that NADH oxidase was a preferred substrate in the heart. Subsequently, the tendency of superoxide production was in accordance with the increase in NAD(P)H oxidase activity, suggesting that NAD(P)H oxidase might be involved in the oxidative stress production and the pathological changes in 2k2C hypertensive rats.

2.6. Expression of NAD(P)H oxidase subunits in 2K2C rats and the effect of tanshinone IIA

There are several isoforms of NAD(P)H oxidase which are believed to be involved in cardiovascular disease. To dissect which one is responsible for Tan IIA induced decrease of oxidative stress production, we performed RT-PCR and Western blotting. As shown in Fig. 4, the mRNA levels of Nox4 and p47phox in the LV and aorta were increased in the 2K2C group compared with those of Sham group, while the mRNA levels of Nox2 was only increased in LV and Nox1 only in the aorta. Tan IIA treatment significantly suppressed the levels of Nox2, Nox4 and p47phox ($P < 0.05$) in both the heart and the aorta, but didn't affect Nox1 in the aorta.

The change tendency of Nox1, Nox2, Nox4 and p47phox protein expression in LV and aorta were in accordance with those of mRNA transcription. As shown in Fig. 5, the Nox4 and p47phox subunit of NAD(P)H oxidase were significantly elevated in both LV and aorta tissues in 2K2C hypertensive rats 10 weeks after operation, while Nox2 expression only was increased in LV and Nox1 only in the aorta. Tan IIA treatment for 6 weeks decreased Nox2, Nox4 and p47phox expression in both the heart and the

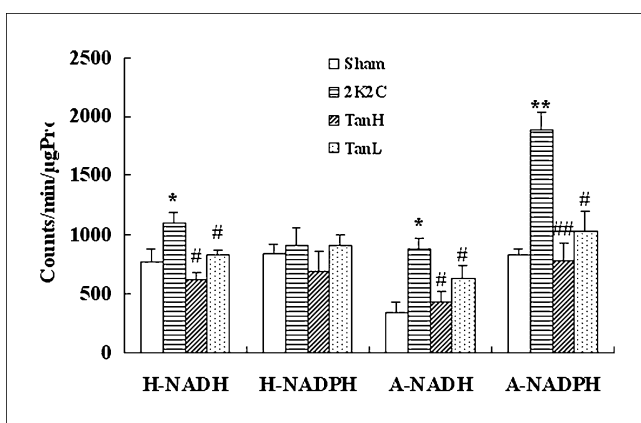


Fig. 3: Changes of NAD(P)H oxidase activity in LV and aorta homogenates determined by chemiluminescence of lucigenin in 2K2C hypertensive rats and the effect of Tan IIA. H-NADH, H-NADPH, A-NADH, A-NADPH, represent NADH and NADPH oxidase activity in LV and aorta respectively; Other abbreviations as above. Data are expressed as means ± SD. * $p < 0.05$ vs. Con., # $p < 0.05$ vs. Mod, n = 6

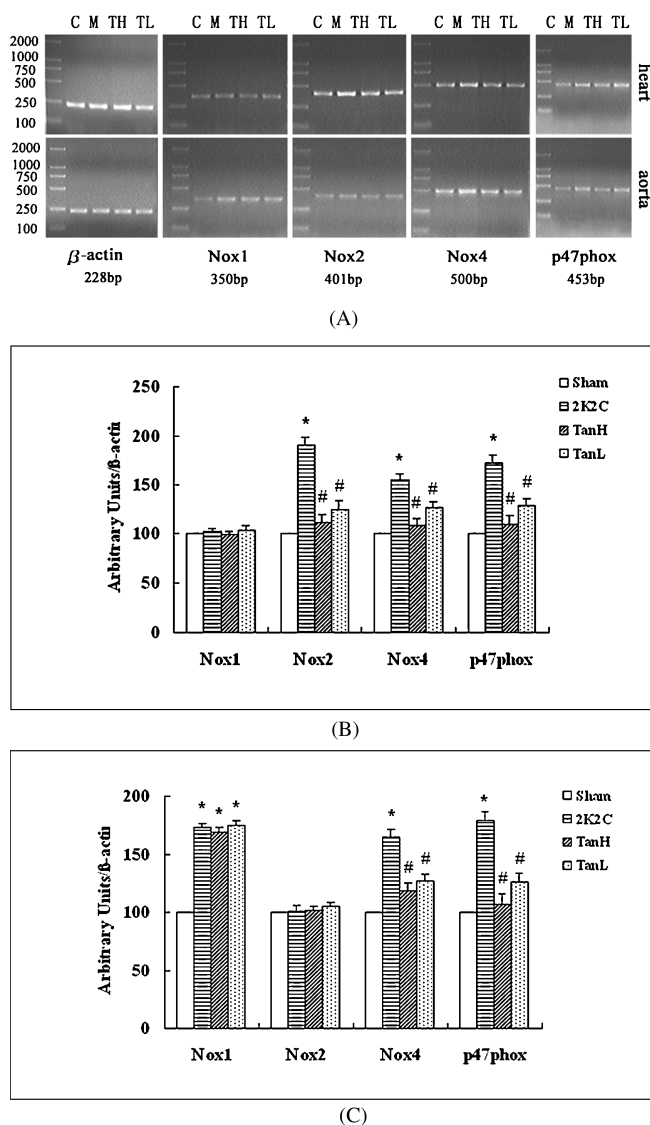


Fig. 4: Effect of Tan IIA treatment on the mRNA expression of Nox1, Nox2, Nox4 and p47phox in LV and aorta of 2K2C rats. (A) Representative PCR band photograph. (B) Ratio of the mRNA expression of Nox1, Nox2, Nox4 and p47phox to β -actin in the LV. (C) Ratio of the mRNA expression of Nox1, Nox2, Nox4 and p47phox to β -actin in the aorta. The data are presented as percentage of optical densities ratio, relative to control conditions. Data are means \pm SD, $n=6$. * $p<0.05$ vs. Con. # $p<0.05$ vs. Mod

aorta but did not affect Nox1 in the aorta. The tissue specificity of different Nox homologues expression might explain why there was different substrate selectivity between LV and aorta, which may contribute to structural and functional abnormalities.

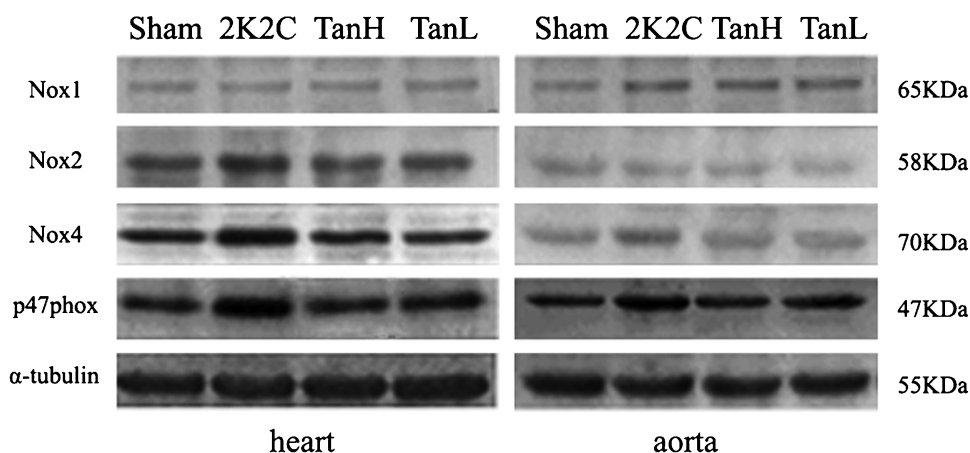
3. Discussion

Hypertension often induces cardiac hypertrophy and fibrosis, which ultimately resulted in chronic heart failure. Much work has been done to understand the mechanism of cardiac remodeling and the methods to regress this process, however there is no effective strategy that prevents cardiac remodeling (Jugdutt 2003). Anti-hypertensive drugs cannot attain ideal cardiovascular-protective effects especially in the decompensated period. Previously, we demonstrated that Tan IIA, the main active diterpene quinone extracted from Danshen which is a traditional medicine and widely used for treating cardiovascular diseases in China, can attenuate atherosclerotic calcification and protect cardiac myocytes against apoptosis due to its antioxidant properties (Fu et al. 2007; Gao et al. 2008; Tang et al. 2007). In this study, we demonstrated that Tan IIA attenuated cardiac

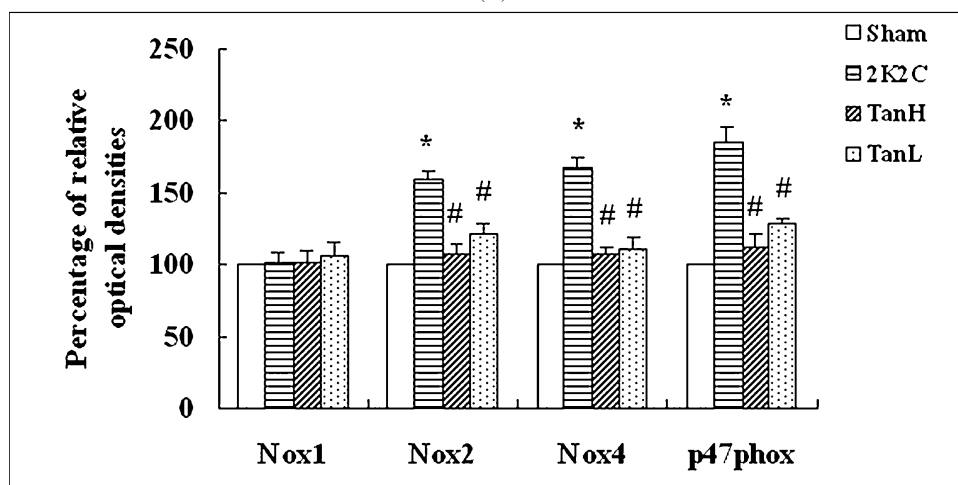
hypertrophy and fibrosis in two-kidney, two-clip (2K2C) renovascular hypertensive rats via inhibiting NAD(P)H oxidases. It is well known that the 2K2C rat model is ideal for studying the role of volume expansion and pressure-overload in the development of hypertension, which represents human renovascular hypertension. Due to the absence of normal kidney function, compensation of sodium and water excretion was weakened, and hence, hypertension occurs in 2K2C rats (Sun and Zhang 2005). Our and other's studies have shown that oxidative stress plays a role in the pathogenesis of myocardial remodeling in various cardiac diseases (Fu et al. 2007; Takimoto and Kass 2007). Redox-sensitive signaling pathways are implicated in the development of cardiac hypertrophy, fibrosis, matrix remodelling, and apoptosis, which can be attenuated by various antioxidant approaches (Berk et al. 2007; Shiomi et al. 2004). In the present study, we demonstrated that superoxide anion was increased in the left ventricle and the aorta of 2K2C rats, which was inhibited by administration of Tan IIA. Tan IIA improve the cardiac function and attenuated cardiac fibrosis in 2K2C rats, however, it did not control blood pressure (BP). These results indicated that Tan IIA treatment might exert cardiac protective effects independent of BP control. There are also similar reports that small dose administration of angiotensin converting enzyme inhibitors (ACEI) resulted in reduced generation of superoxide anion and inhibited cardiac fibrosis in the SHRSP heart independent of BP lowering (Liao et al. 2004; Rugale et al. 2005).

The NADPH oxidase family is now well recognized as a major source of ROS involved in cardiovascular pathophysiology (Bedard and Krause 2007). Recent studies in gene-modified mice and in human heart failure (Johar et al. 2006; Looi et al. 2008) support an involvement of NADPH oxidase in cardiac remodeling. To investigate the mechanism by which Tan IIA decreased $O_2^{\bullet-}$ production we examined the effect of Tan IIA on vascular NAD(P)H oxidases. In the present study, NADH oxidase activity was elevated in LV and aorta in 2K2C hypertensive rats and Tan IIA alleviated these effects, which might contribute to its anti-oxidative effects and the protective effect against cardiac remodeling *in vivo*. Interestingly, NADPH oxidase activity in the LV showed no significant change among individual groups. There are two possibilities: 1) NADH oxidase was a preferred substrate in the heart; 2) vascular NADPH was endocrined to the blood from the vessel and exert its effect in the heart. Subsequently, the tendency of superoxide production was in accordance with the increase of NAD(P)H oxidase activity, suggesting that NAD(P)H oxidase might be responsible for the reduced oxidative stress after Tan IIA administration in 2k2C hypertensive rats.

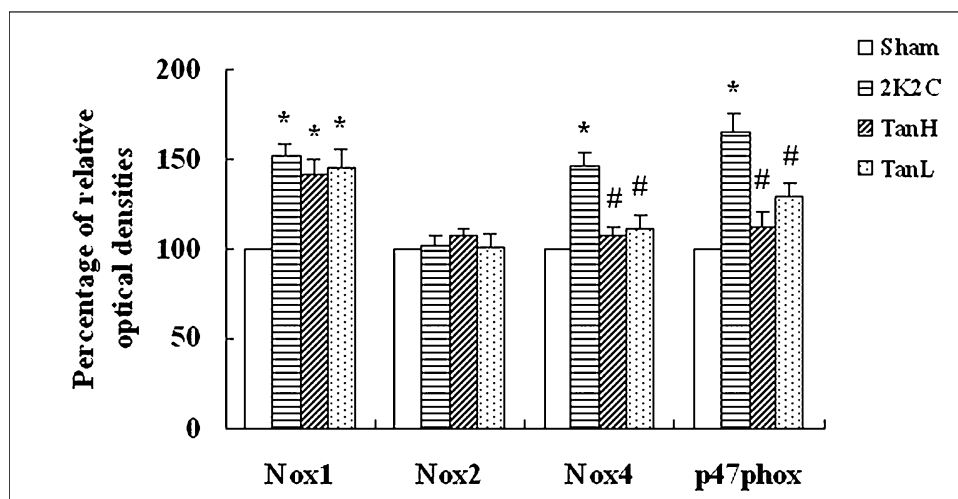
In neutrophils, NAD(P)H oxidase consists of a core heterodimer comprising the electron transferring plasma membrane subunits p22phox and gp91phox (or nox2) and 4 cytosolic subunits (p40phox, p47phox, p67phox, and the small G-proteinrac1/2), which provide regulatory function (Griendling et al. 2000). In vascular smooth muscle and endothelial cells, gp91phox (Nox2) coexists with other homologues termed nox1 and nox4 (Ago et al. 2004), whereas Nox2 containing NAD(P)H oxidase is the most common isoform in the human ventricular myocardium (Lassegue et al. 2001; Sorescu et al. 2002). In the present study, both Nox2, Nox4 and p47phox expression were increased in the heart indicating that both Nox2 and Nox4 containing NAD(P)H oxidase may contribute to the production of oxidative stress in 2K2C rats. Individual Nox isoforms may differ in the effect they have on cardiovascular remodeling in response to complex stimulus (Byrne et al. 2003). Prior studies in mice lacking Nox2 or p47phox (which is necessary for Nox2 activation) suggest that this isoform is especially important for cardiac remodeling (Bendall et al. 2002; Wang et al.), although *in vitro* studies in cultured fibroblasts have also implicated Nox4 in the transfor-



(A)



(B)



(C)

Fig. 5: Effect of Tan IIA treatment on the expression of Nox1, Nox2, Nox4 and p47phox in LV and aorta of 2K2C rats. (A) Original Western blots representing the similar results of 6–10 rats. Equal protein loading was verified by α -tubulin immunostaining. (B, C) Densitometric quantification of Western blots in LV and aorta respectively. The values from experiment groups have been normalized to values in sham group (Minuz et al.). Data are means \pm SD, $n=6$. * $p < 0.05$ vs. Con. # $p < 0.05$ vs. Mod

mation of fibroblasts to myofibroblasts (Cucoranu et al. 2005). It was recently reported that in cultured human cardiac fibroblasts TGF β -1 promoted transformation into myofibroblasts and the expression of smooth muscle α -actin in a Nox4-dependent manner (Cucoranu et al. 2005). These observations suggest that the different subunits of NAD(P)H oxidase may mediate varied effects on cardiac remodeling. In our study Tan IIA may exert the cardioprotective effect through its inhibitory action on both Nox2 and Nox4 containing NAD(P)H oxidase.

We also observed stimulus-specific and isoform-specific roles in aorta. The Nox-based NAD(P)H oxidases served different functions in the vasculature. Nox1 and Nox4 were expressed in VSMC, whereas fibroblasts contained Nox2. Nox1 may produce large amounts of $O_2^{\bullet-}$ when required (important for growth), whereas Nox4 may mediate a steady production of low amounts of $O_2^{\bullet-}$ that were important in the metabolic and differentiation functions of the cell. But Szocs and Cowosrer found that Nox1 mRNAs was increased 2.7-fold at day 3 after balloon injury in

rat carotid artery and remained elevated for 15 days (Sorescu et al. 2002). Nox2 was increased 7 to 15 days after injury, and Nox4 expression was increased 2-fold, but only at day 15 after surgery. Wendt et al. found a doubling in Nox1 protein expression, while the expression of Nox4 remained unchanged in aorta eight weeks after streptozotocin treatment (Albers and Beal 2002). In the present study, the expression of Nox1 and Nox4 increased in aorta in 2K2C hypertensive rats. Tan IIA normalized Nox4 expression but had no effect on Nox1. Tan IIA produced different effect on cardiovascular remodeling and BP maybe through its selectivity of action on different Nox homologues. In summary, chronic treatment with Tan IIA improved cardiac dysfunction and attenuated cardiovascular remodeling in 2K2C rats. This might be ascribed to the inhibitory effect of Tan IIA on NAD(P)H oxidase-derived ROS and redox-signaling independent of blood pressure (BP) control. Although further studies to elucidate the primary mechanisms remain to be performed, this work provides the potential clues to understand the important therapeutic implications of Tan IIA on cardiac remodeling in renovascular hypertension.

4. Experimental

4.1. Animals and experimental protocol

Male Sprague-Dawley rats were obtained from the Center of Experimental Animal Sun Yat-sen University (Guangzhou, China). All the animal experimental procedures were approved by the Institutional Animal Care and Use Committee of Sun Yat-sen University and complied with the National Institutes of Health Guide for the Care and Use of Laboratory Animals. All rats had free access to standard chow and water and were housed under controlled environment conditions (12 h light/dark cycle and room temperature $22 \pm 1^\circ\text{C}$).

Renovascular hypertension was induced in rats using the method established in our laboratory (Zhou et al. 2006). Briefly, male Sprague-Dawley rats (90–110 g) were anaesthetized using sodium pentobarbital (30 mg kg^{-1} i.p.). After a midline laparotomy, one silver clip with an internal diameter of 0.30 mm was placed around the left and right renal artery, respectively. Sham-operated rats, which underwent the same surgical procedure except for the placement of the renal artery clip, served as controls.

Body weight, heart rate and systolic blood pressure (SBP) were measured once every two weeks. Noninvasive SBP was measured in nonanaesthetized animals and rats were considered to be hypertensive when SBP was higher than 160 mmHg as described earlier (Zhou et al. 2006). After 4 weeks the hypertensive 2K2C rats were divided into untreated (2K2C) and Tan IIA-treated (TanH and TanL) groups. Tan IIA (70 mg kg^{-1} and 35 mg kg^{-1} per day, respectively, mixed with 0.5% carboxymethyl cellulose sodium) were given by gastric gavages once a day for 6 weeks. The sham-operated rats (Sham) were orally given vehicle (0.5% carboxymethyl cellulose sodium), which served as controls. At 10 weeks after surgery, the rats are sacrificed and we harvested heart and aorta tissues.

4.2. Echocardiographic and hemodynamic analyses

Transthoracic echocardiographic studies were performed on rats before operation, before treatment and 1 day before sacrifice with MPX DU8 (Technos, Italy), as previously described in detail (Zhou et al. 2006). In brief, rats were anesthetized with sodium pentobarbital (30 mg kg^{-1} i.p.). The two-dimensional short-axis view of the left ventricle and M-mode tracings were recorded through the intraventricular septum and posterior LV walls at the papillary muscle level to measure LV end-diastolic dimension, fractional shortening, and LV ejection fraction. All Doppler spectra were recorded on paper at 100 mm s^{-1} and analyzed off-line.

Rats of each group were anesthetized with sodium pentobarbital (30 mg kg^{-1} i.p.) after the administration for 6 weeks. LV hemodynamic studies were performed by cannulation of the right carotid artery with a polyethylene Millar Pressure Catheter that was carefully advanced to the LV (Zhou et al. 2006).

4.3. Histochemistry and collagen quantification

Blood was chased from major vessels by whole-body perfusion of saline solution through the heart, followed by *in situ* organ fixation using 40 mL Bouin fixative solution (0.9% picric acid, 10% formaldehyde, and 5% glacial acetic acid). Organs were quickly removed and postfixed for 5 h. Fixed tissue was stored in 70% ethanol at 4°C until analyzed.

Tissues were dehydrated, embedded in paraffin blocks, cut into $5\text{ }\mu\text{m}$ sections, and mounted on 3-aminopropyltriethoxysilane-coated slides. Sections were deparaffinized, rehydrated, and washed with H_2O . The cardiac sections were stained with VG staining for assessment of interstitial and perivascular collagen content. Quantification of fibrosis was performed using an image analysis system (Northern Eclipse 5.0; EM-PIX Imaging Inc). A single investigator unaware of the nature of the experimental groups performed the analysis.

4.4. Measurement of $\text{O}_2^{\bullet-}$ production and NAD(P)H oxidase activity by lucigenin-enhanced chemiluminescence

The $\text{O}_2^{\bullet-}$ production of LV and aorta was estimated with lucigenin-enhanced chemiluminescence. LV and aortic segments were placed in chilled modified Krebs/HEPES buffer and homogenized on ice with a glass/glass tissue homogenizer for 2 min. in 50 mmol/L PBS which contained 0.01 mmol/L EDTA. The homogenate was centrifuged at 10000 g for 20 min. The pellet was discarded, and the protein content of supernatant was determined by the method of Bradford (Bio-Rad). After 5 min. of dark adaptation, scintillation vials containing 2 mL Krebs-HEPES buffer with $5\text{ }\mu\text{mol/L}$ lucigenin and $25\text{ }\mu\text{g}$ protein were placed into a luminometer (TD-20/20; Turner Designs, Sunnyvale, CA, USA). Luminescence measurements were integrated for 30-s periods, and the cycle was repeated 9 times; the 10 values were then averaged. After 10 cycles, the cell-permeant $\text{O}_2^{\bullet-}$ scavenger Tiron (10 mM) was added, and 15 more cycles were read; the final 8 values, which appeared to be maximally reduced, were averaged. Data were calculated as the change in the rate of luminescence per minute per microgram of protein of values before and after Tiron and then converted to $\text{O}_2^{\bullet-}$ (RLU/min/ μg protein) as described previously (Cifuentes et al. 2000).

The LV and aorta were washed with ice-cold PBS and homogenized in cold lysis buffer (contain protease inhibitors). NAD(P)H oxidase activity was measured by a luminescence assay in a 50 mmol/L phosphate buffer, pH 7.0, containing 1 mmol/L EGTA, 150 mmol/L sucrose, $5\text{ }\mu\text{mol/L}$ dark-adapted lucigenin as the electron acceptor, and 100 $\mu\text{mol/L}$ NADH or NADPH as the substrate in a final volume of 900 μL . The reaction was started by the addition of 100 μL of homogenate, and luminescence measurements were obtained every 15 s for 5 min. Protein content was determined in an aliquot of the homogenate. The results were measured as the rate of photon counts per microgram protein following subtraction of the counts obtained from a buffer blank (Jalil et al. 2005).

4.5. Reverse transcription-polymerase chain reaction analysis

Total RNA was isolated from the frozen left ventricles and aortas using TRIzol reagent according to the manufacturer's instructions (Invitrogen, Carlsbad, CA). Total RNA (0.5– $1\mu\text{g}$) was reverse transcribed and amplified using the Titan One Tube RT-PCR system (Roche Applied Science, Indianapolis, IN) using the oligonucleotide primers shown in Table 1. Following reverse transcription and PCR the amplicons were separated on 2% agarose gels, stained with ethidium bromide and photographed.

4.6. Western blot analysis

Immunoblots were basically performed as previously described (Zhang et al. 2007). The isolated LV and aorta were quickly frozen in liquid nitrogen, and homogenized with a motorized homogenizer in ice-cold lysis buffer containing protease inhibitors (50 mmol/L Tris/HCl, pH 7.4, 1 mmol/L EDTA, 500 mmol/L phenylmethyl-sulfonyl fluoride (PMSF), 2 mmol/L leupeptin, and 10 mg/mL aprotinin), centrifuged, then the supernatants were collected. Protein concentrations were determined by the method of Bradford (Bio-Rad, Hercules, CA, USA). Equal amounts of protein (40 μg protein per lane) were separated by 12% SDS-PAGE and then transferred onto PVDF membranes (Bio-Rad, Hercules, CA, USA). Blocking solution (5% skim milk) was loaded over membranes for 1 h at room temperature. The membranes were incubated with anti-p47phox (1:200 dilution, Santa Cruz, CA, USA), anti-Nox2 (1:200 dilution, Santa Cruz, CA, USA), anti-Nox4 (1:200 dilution, Santa Cruz, CA, USA) overnight at 4°C and with anti- α -tubulin (1:10,000 dilution, Sigma) for 1 h at room temperature. Then horseradish peroxidase (HRP)-labeled secondary immunoglobulin antibodies (1:2000 dilution, Cell Signaling) were added for 1 h at room temperature. The signals were detected by the enhanced chemiluminescence method (Amersham). After immunoblotting, the film was scanned and densitometric analyses were performed using NIH Image software (ver. 1.62).

4.7. Statistical analysis

Data are expressed as means \pm SEM. Unpaired *t* test, 1-factor ANOVA followed by Student-Newman-Keuls test, and linear correlation tests were used. A *P* value < 0.05 was considered statistically significant.

Acknowledgments: This study was supported by research grants: National Natural Science Foundation of China (No. 30772576), NSFC-CIHR (No. 30811120434), the National Science and Technology Major Project of China “Key New Drug Creation and Manufacturing Program” (Grant 2009ZX09102-152, 2009ZX09303-007), Major Program of Guangzhou City (P. R. of China, No.2006-Z2-E-4022), Major Program in Key Field of People’s Government of Guangdong Province, China (No:2003A30904); Key Program of Ministry of Education, China (No: 104146); Key Natural Science Fund of Guangdong province, China (No: 04105349); Key Program of Guangdong Province, China (No: 2003B31713) and Key Program of Guangzhou city, China (No:2003Z1-E5011)

References

- Ago T, Kitazono T, Ooboshi H, Iyama T, Han YH, Takada J, Wakisaka M, Ibayashi S, Utsumi H, Iida M (2004) Nox4 as the major catalytic component of an endothelial NAD(P)H oxidase. *Circulation* 109: 227–233.
- Albers DS, Beal MF (2002) Mitochondrial dysfunction in progressive supranuclear palsy. *Neurochem Int* 40: 559–564.
- Bedard K, Krause KH (2007) The NOX family of ROS-generating NADPH oxidases: physiology and pathophysiology. *Physiol Rev* 87: 245–313.
- Bendall JK, Cave AC, Heymes C, Gall N, Shah AM (2002) Pivotal role of a gp91 (phox)-containing NADPH oxidase in angiotensin II-induced cardiac hypertrophy in mice. *Circulation* 105: 293–296.
- Berk BC, Fujiwara K, Lehoux S (2007) ECM remodeling in hypertensive heart disease. *J Clin Invest* 117: 568–575.
- Byrne JA, Grieve DJ, Bendall JK, Li JM, Gove C, Lambeth JD, Cave AC, Shah AM (2003) Contrasting roles of NADPH oxidase isoforms in pressure-overload versus angiotensin II-induced cardiac hypertrophy. *Circ Res* 93: 802–805.
- Cifuentes ME, Rey FE, Carretero OA, Pagano PG (2000) Upregulation of p67 (phox) and gp91 (phox) in aortas from angiotensin II-infused mice. *Am J Physiol Heart Circ Physiol* 279: H2234–2240.
- Cucoranu I, Clempus R, Dikalova A, Phelan PJ, Ariyan S, Dikalov S, Sorescu D (2005) NAD(P)H oxidase 4 mediates transforming growth factor-beta1-induced differentiation of cardiac fibroblasts into myofibroblasts. *Circ Res* 97: 900–907.
- Ertl G, Frantz S (2005) Healing after myocardial infarction. *Cardiovasc Res* 66: 22–32.
- Fu J, Huang H, Liu J, Pi R, Chen J, Liu P (2007) Tanshinone IIA protects cardiac myocytes against oxidative stress-triggered damage and apoptosis. *Eur J Pharmacol* 568: 213–221.
- Gao J, Yang G, Pi R, Li R, Wang P, Zhang H, Le K, Chen S, Liu P (2008) Tanshinone IIA protects neonatal rat cardiomyocytes from adriamycin-induced apoptosis. *Transl Res* 151: 79–87.
- Griendling KK, Sorescu D, Ushio-Fukai M (2000) NAD(P)H oxidase: role in cardiovascular biology and disease. *Circ Res* 86: 494–501.
- Hare JM (2001) Oxidative stress and apoptosis in heart failure progression. *Circ Res* 89: 198–200.
- Jalil JE, Perez A, Ocaranza MP, Bargetto J, Galaz A, Lavandero S (2005) Increased aortic NADPH oxidase activity in rats with genetically high angiotensin-converting enzyme levels. *Hypertension* 46: 1362–1367.
- Johar S, Cave AC, Narayanapanicker A, Grieve DJ, Shah AM (2006) Aldosterone mediates angiotensin II-induced interstitial cardiac fibrosis via a Nox2-containing NADPH oxidase. *FASEB J* 20: 1546–1548.
- Jugdutt BI (2003) Ventricular remodeling after infarction and the extracellular collagen matrix: when is enough enough? *Circulation* 108: 1395–1403.
- Khaper N, Kaur K, Li T, Farahmand F, Singal PK (2003) Antioxidant enzyme gene expression in congestive heart failure following myocardial infarction. *Mol Cell Biochem* 251: 9–15.
- Lambeth JD (2004) NOX enzymes and the biology of reactive oxygen. *Nat Rev Immunol* 4: 181–189.
- Lassegue B, Clempus RE (2003) Vascular NAD(P)H oxidases: specific features, expression, and regulation. *Am J Physiol Regul Integr Comp Physiol* 285: R277–R279.
- Lassegue B, Sorescu D, Szocs K, Yin Q, Akers M, Zhang Y, Grant SL, Lambeth JD, Griendling KK (2001) Novel gp91 (phox) homologues in vascular smooth muscle cells: nox1 mediates angiotensin II-induced superoxide formation and redox-sensitive signaling pathways. *Circ Res* 88: 888–894.
- Liao Y, Asakura M, Takashima S, Ogai A, Asano Y, Shintani Y, Minamino T, Asanuma H, Sanada S, Kim J, Kitamura S, Tomoike H, Hori M, Kitakaze M (2004) Celiprolol, a vasodilatory beta-blocker, inhibits pressure overload-induced cardiac hypertrophy and prevents the transition to heart failure via nitric oxide-dependent mechanisms in mice. *Circulation* 110: 692–699.
- Looi YH, Grieve DJ, Siva A, Walker SJ, Anilkumar N, Cave AC, Marber M, Monaghan MJ, Shah AM (2008) Involvement of Nox2 NADPH oxidase in adverse cardiac remodeling after myocardial infarction. *Hypertension* 51: 319–325.
- Lu L, Quinn MT, Sun Y (2004) Oxidative stress in the infarcted heart: role of de novo angiotensin II production. *Biochem Biophys Res Commun* 325: 943–951.
- Minuz P, Patrignani P, Gaino S, Degan M, Menapace L, Tommasoli R, Seta F, Capone ML, Tacconelli S, Palatresi S, Bencini C, Del Vecchio C, Mansueto G, Arosio E, Santonastaso CL, Lechi A, Morganti A, Patrono C (2002) Increased oxidative stress and platelet activation in patients with hypertension and renovascular disease. *Circulation* 106: 2800–2805.
- Murdoch CE, Zhang M, Cave AC, Shah AM (2006) NADPH oxidase-dependent redox signalling in cardiac hypertrophy, remodelling and failure. *Cardiovasc Res* 71: 208–215.
- Nakagami H, Takemoto M, Liao JK (2003) NADPH oxidase-derived superoxide anion mediates angiotensin II-induced cardiac hypertrophy. *J Mol Cell Cardiol* 35: 851–859.
- Rugale C, Cordaillat M, Mimran A, Jover B (2005) Prevention and reversal by enalapril of target organ damage in angiotensin II hypertension. *J Renin Angiotensin Aldosterone Syst* 6: 154–160.
- Shiomi T, Tsutsui H, Matsusaka H, Murakami K, Hayashidani S, Ikeuchi M, Wen J, Kubota T, Utsumi H, Takeshita A (2004) Overexpression of glutathione peroxidase prevents left ventricular remodeling and failure after myocardial infarction in mice. *Circulation* 109: 544–549.
- Sorescu D, Weiss D, Lassegue B, Clempus RE, Szocs K, Sorescu GP, Valppu L, Quinn MT, Lambeth JD, Vega JD, Taylor WR, Griendling KK (2002) Superoxide production and expression of nox family proteins in human atherosclerosis. *Circulation* 105: 1429–1435.
- Sun ZJ, Zhang ZE (2005) Historic perspectives and recent advances in major animal models of hypertension. *Acta Pharmacol Sin* 26: 295–301.
- Takahashi K, Ouyang X, Komatsu K, Nakamura N, Hattori M, Baba A, Azuma J (2002) Sodium tanshinone IIA sulfonate derived from Danshen (*Salvia miltiorrhiza*) attenuates hypertrophy induced by angiotensin II in cultured neonatal rat cardiac cells. *Biochem Pharmacol* 64: 745–749.
- Takimoto E, Kass DA (2007) Role of oxidative stress in cardiac hypertrophy and remodeling. *Hypertension* 49: 241–248.
- Tang F, Wu X, Wang T, Wang P, Li R, Zhang H, Gao J, Chen S, Bao L, Huang H, Liu P (2007) Tanshinone IIA attenuates atherosclerotic calcification in rat model by inhibition of oxidative stress. *Vascul Pharmacol* 46: 427–438.
- Wang M, Zhang J, Walker SJ, Dworakowski R, Lakatta EG, Shah AM (2010) Involvement of NADPH oxidase in age-associated cardiac remodeling. *J Mol Cell Cardiol* 48: 765–772.
- Weber KT (1997) Extracellular matrix remodeling in heart failure: a role for de novo angiotensin II generation. *Circulation* 96: 4065–4082.
- Zhang H, Pi R, Li R, Wang P, Tang F, Zhou S, Gao J, Jiang J, Chen S, Liu P (2007) PPARbeta/delta activation inhibits angiotensin II-induced collagen type I expression in rat cardiac fibroblasts. *Arch Biochem Biophys* 460: 25–32.
- Zhou G, Jiang W, Zhao Y, Ma G, Xin W, Yin J, Zhao B (2003) Sodium tanshinone IIA sulfonate mediates electron transfer reaction in rat heart mitochondria. *Biochem Pharmacol* 65: 51–57.
- Zhou SG, Zhou SF, Huang HQ, Chen JW, Huang M, Liu PQ (2006) Proteomic analysis of hypertrophied myocardial protein patterns in renovascularly hypertensive and spontaneously hypertensive rats. *J Proteome Res* 5: 2901–2908.